Research Paper

Multi-sensor measurement of O_2, CO_2 and reheating in triticale silage: An extended approach from aerobic stability to aerobic microbial respiration

Guilin Shan [a,1], Christian Maack [a], Wolfgang Buescher [a], Gereon Glenz [b], Andreas Milimonka [b], Hauke Deeken [a], David A. Grantz [c], Ye Wang [a], Yurui Sun [a,*,1]

[a] Department of Agricultural Engineering, The University of Bonn, 53115, Bonn, Germany
[b] ADDCON GmbH, 06749, Bitterfeld-Wolfen, Germany
[c] Department of Botany & Plant Sciences, University of California at Riverside, Parlier, CA, 93648, United States

ARTICLE INFO

The biochemical reactions of aerobic microbial respiration (AMR) suggest that silage temperature (T_{si}) rise, oxygen (O_2) consumption and carbon dioxide (CO_2) emission may be equally useful as indicators of silage deterioration during feed-out, but only temperature has been used extensively to assess aerobic stability. Here we extend the study of aerobic stability to incorporate AMR of silage by developing a novel experimental cell integrated with multiple sensors. Silage samples, ensiled from a triticale crop, were made in twelve air-tight barrels (60 L), packed to bulk densities of 190 or 250 kg m^{-3} dry matter (DM). T_{si} and O_2 measurements were co-located at 15- and 30-cm behind the working face. CO_2 was measured as flux across the working face. The experimental period of aerobic exposure was 7 days. We provide the first reports of: (i) distinct aerobic responses of these parameters, showing that T_{si} varied with CO_2 in phase but with O_2 out-of phase; (ii) CO_2 flux was dominated initially by anaerobic discharge and subsequently by aerobic products; (iii) linear relationships between aerobic reheating and both O_2 consumption ($0.994 \geq R^2 \geq 0.815$, $P < 0.01$) and CO_2 flux ($0.981 \geq R^2 \geq 0.464$, $P < 0.01$); and (iv) variable magnitude of daily aerobic production of CO_2 per kg DM from 2.3 to 133.4 mmol kg d^{-1}. These results demonstrate that the novel multi-sensor technique has powerful capacity to provide insight into AMR of silage and thus provide more detailed information to guide silage management than previous measurements of aerobic stability.

---

* Corresponding author.
  E-mail addresses: pal@cau.edu.cn, ysun@uni-bonn.de (Y. Sun).
  [1] These authors contributed equally to this work.

Nomenclature

AI	Active ingredient
AMR	Aerobic microbial respiration
AP_{CO_2}	Aerobic CO_2 production, mmol kg^{-1}
B	Bulk density, kg m^{-3}
CO_2	Carbon dioxide
cfu	Colony forming units
DM	Dry matter
HD	High density
LD	Low density
M	The DM of silage in the barrel, kg
NDIR	Nondispersive infrared
O_2	Oxygen
P	Statistical significance
P_{atm}	Atmospheric pressure, Pa
R	Universal gas constant, 8.314 m^3 Pa K^{-1} mol^{-1}
R^2	Coefficient of determination
S	The exposed silage face area, m^2
SEM	Standard error of the mean
T_a	Ambient temperature, K
Tr	Treatment
T_{si}	Silage temperature, °C
t	Time, h
t_o	Initial time, h
V	The volume of the gas chamber, m^3
WW	Wet mass
J_{CO_2}	The flux of CO_2, mol m^{-2} h^{-1}
ρ	The porosity of the silage
$[CO_2]$	CO_2 concentration, ppm
$\Delta[CO_2]$	The change in CO_2 concentration, ppm
ΔO_2	The decline of oxygen, vol. %
ΔT_{si}	Difference between T_{si} and T_a, °C
Δt	The difference in time, h

1. Introduction

Silage is one of the most important global feedstuffs and is a major substrate of biogas production (Herrmann, Idler, & Heiermann, 2015; Herrmann, Prochnow, & Heiermann, 2011; Wilkinson & Muck, 2019). However, aerobic deterioration during feed-out of silage, when the silo is opened to the air, causes unavoidable losses, though these can be mitigated with informed management practices (Borreani, Tabacco, Schmidt, Holmes, & Muck, 2018; Honig, 1990; Pahlow, Muck, Driehuis, Elferink, & Spoelstra, 2003; Pitt & Muck, 1993; Wilkinson & Davies, 2013).

Silage losses are caused by a variety of spoilage microorganisms that metabolise residual sugar, lactic acid, and other organic acids. Based on the biochemical reactions of aerobic microbial respiration (AMR), temperature (T_{si}), oxygen (O_2) consumption and carbon dioxide (CO_2) emission in silage have been suggested as indicators of aerobic deterioration (Courtin & Spoelstra, 1990; Honig, 1990). Among these parameters T_{si} has been widely used, due to ease of measurement, with a parameter variously defined as the time after opening for silage temperature (T_{si}) to reach 1.7 °C (Johnson et al., 2002), 2 °C (Muck, 2004; Ranjit & Kung, 2000; Wilkinson & Davies, 2013), 2.5 °C (Kristensen et al., 2010) or 3 °C above ambient temperature (T_a) (Herrmann et al., 2015; Jatkauskas, Vrotniakiene, Ohlsson, & Lund, 2013; Weiss, Kroschewski, & Auerbach, 2016). In contrast, continuous and simultaneous measurement of O_2 influx and CO_2 outflow are methodologically more complicated, generally determined by gas extraction from silage followed by off-line analysis using gas chromatography (Lee, Hanna, & Bullerman, 1986; McEniry, Forristal, & O'Kiely, 2011; Weinberg & Ashbell, 1994; Williams, Hoxey, & Lowe, 1997) or by chemical titration with hydrochloric acid (HCl) solution (Ashbell, Weinberg, Azrieli, Hen, & Horev, 1991; Ashbell, Weinberg, Hen, & Filya, 2002; Weinberg, Chen, & Solomon, 2009). These analytical methods are logistically restricted to daily measurements, missing more dynamic information about microbial activity and oxidation rates. In addition, gas extraction may disturb the integrity of the silage (Muck & Pitt, 1994).

Silage is a porous material, containing both air- and water-filled pores (Muck & Pitt, 1994). At the opening face of the silo, gas fluxes of O_2 and CO_2 are in opposite directions, i.e. O_2 inward and CO_2 outward. Accurate measurement of these parameters relies on biochemical and microbial fundamentals for silage production, physical characteristics of porous media, gas transfer mechanisms (concentration diffusion modelled by Fick's law and advective flow by Darcy's law) in silage, and the technical properties of relevant sensors and novel instrument design. Over the last decade, several O_2 and CO_2 sensors have been suggested for silage research (Green et al., 2012; Shan, Buescher, Maack, Zhou, & Sun, 2019; Shan et al., 2016; Sun et al., 2015). To our knowledge, a comprehensive study with O_2, CO_2 and T_{si} to observe AMR of silage using a multi-sensor fusion method remains lacking, but may contribute to development of an optimal marker of aerobic deterioration for silage management. Recently, Wilkinson and Muck (2019) suggested that an early indicator that silage is aerobically unstable, and likely to show substantial spoilage within 24 h, occurs when lactate-assimilating yeast counts are $>10^5$ cfu g^{-1} [silage]. Once yeast populations reach ~10^7 cfu g^{-1} [silage], silage pH and temperature begin to increase. Since sending samples to a forage testing laboratory for plate-culture yeast counts can take several days, an early indicator of aerobic deterioration that can be measured in real time is needed, and requires the development of novel instruments.

The objectives of this study were (i) to develop an experimental system incorporating a multi-sensor approach for monitoring AMR by measurement of O_2, CO_2 and T_{si} during feed-out of silage, (ii) to determine the aerobic characteristics of these three diagnostic parameters in response to air exposure at the working face, (iii) to investigate the interrelation of these parameters and their individual or combined utility as indicators of aerobic stability.

2. Materials and methods

2.1. Research fundamental

Well-produced silage contains a high content of lactic acid, and relatively lower contents of acetic acid, ethanol and

carbohydrate (Filya, 2003; Kung, Shaver, Grant, & Schmidt, 2018; Robinson & Swanepoel, 2016). Table 1 summarises the aerobic respiratory equations relevant to these components and chemical reactions associated with the by-products and roles of microorganisms in silage (Courtin & Spoelstra, 1990; Muck, 2004). As the by-product of aerobic metabolism, CO_2 is created directly from lactic acid ($CH_3CHOHCOOH$), acetic acid (CH_3COOH) and glucose ($C_6H_{12}O_6$), whereas ethanol (C_2H_5OH) in silage is converted first into acetic acid and then reconverted into CO_2. However, even though acetic acid in silage is commonly the second major component of organic acids, it is volatile and thus only a minor fraction is metabolised to CO_2 (Kung et al., 2018). Since the contents of ethanol and residual sugar in well-produced silage are also very low (Bernardes et al., 2018; Borreani et al., 2018; Pahlow et al., 2003), it is assumed that the CO_2 emission from the working face of silage is mainly proportional to the oxidative loss of the lactic acid.

2.2. Multi-sensor experimental cell

The novel experimental cell (Fig. 1a) consists of two parts, a gas chamber for CO_2 flux measurement and a barrel (inner diameter, 35.7 cm; length, 60 cm; volume, 60 L) filled with a silage sample as a mini-silo. These are connected through a band-clamp with rubber O-ring (diameter 35 cm). The gas chamber containing a CO_2 sensor had a mobile lid of aluminium plate (thickness of lid: 1 mm). Opening/closing of the lid was driven by two pneumatic actuators (Mini-cylinder: EM-IA25 × 125-S; stroke length and resultant lid to base separation of 0–12.5 cm; Solenoid valve: EMRV5211-06Q-E4, Zhejiang Eternal Automation Sci-Tec Co., Ltd, Ningbo, China). In the barrel/mini-silo, O_2 and temperature sensors were installed together at two depths (15- and 30-cm behind the silage face). Table 2 lists general information of all types of sensor in the cell. In addition, a metallic net between the silage face and the gas chamber was inserted to prevent the exposed surface from crumbling while allowing exposure to atmospheric oxygen. The experiment layout (Fig. 1b) shows three instrumented cells for triple replication. All barrels/mini-silos were wrapped tightly with insulating phenolic foam (thickness: 3 cm; thermal conductivity: 0.04 W m^{-1} K^{-1}). The experiment was conducted under laboratory conditions that reduced the influence of diurnal variation of ambient temperature. Each cell contained a microchip-based controller/data logger (Flash, 8 MB, 24-channel, 12-bit ADC, 0–2.5 V range, 2-channel RS-232, manufactured in our laboratory). Throughout the experiment, data were logged at 30-min intervals, during which time the mobile lid was opened (27 min) for O_2 diffusion to the silage and then closed (3 min) for measuring CO_2 flux.

2.3. Measurement of CO_2 flux

For measuring CO_2 flux, a nondispersive infrared (NDIR) sensor was used. Its physical structure (Fig. 1c) is composed of a pulse-driven infrared emitter as light source, a perforated pipe for gas sampling and a pair of IR detectors (each having a filter at a specific waveband) to yield a differential signal of CO_2 concentration [CO_2], measured at the wavelength of 4.26 μm. As a function of time (t), the flux of CO_2 (J_{CO_2}) is defined as (Schwendenmann & Macinnis-Ng, 2016)

$$J_{CO_2}(t) = \frac{\Delta[CO_2]}{\Delta t} \cdot \frac{V \cdot P_{atm}}{R \cdot T_a \cdot S \cdot \rho} \tag{1}$$

where $\Delta[CO_2]/\Delta t$ refers to the change in CO_2 concentration within Δt after the mobile lid has been moved to the closed state (i.e. $\Delta t = 0.05$ h), calculated as the slope of the linear function (μmol mol^{-1} h^{-1} = ppm h^{-1}); S is the exposed silage face area (m^2) including the effect of the metallic net between the silage face and the gas chamber (Fig. 1a), ρ is the porosity of the silage, the volume of voids per unit total volume (Pitt, 1986). P_{atm} is atmospheric pressure (Pa), V is the volume of the gas chamber (m^3), and R is the universal gas constant (8.314 m^3 Pa K^{-1} mol^{-1}).

For quantitative comparison of the accumulated CO_2 emission between the low density (LD) and high density (HD) samples, the specific aerobic CO_2 production (AP_{CO_2}) per kg silage DM from initial time (t_o) to arbitrary time (t) was calculated as

$$AP_{CO_2}(t) = \frac{1}{M} \int_{t_o}^{t} S \times J_{CO_2} dt \tag{2}$$

where M (kg) is the DM of silage in the barrel.

2.4. O_2 sensor

The principle of the electrochemical sensor for O_2 measurement (Fig. 1d) is based on an oxidation–reduction reaction that involves a transfer of electrons between two chemical electrodes, an anode (base metal: lead) and a cathode (gold film), immersed in an electrolyte solution (H_2SO_4). The sensor is kept upright to ensure that both electrodes are in contact with the electrolyte solution. When O_2 diffuses into the sensor, a quantitative reduction of O_2 occurs at the cathode ($O_2 + 4H^+ + 4e^- \rightarrow 2H_2O$). Consequently, as the electrons required for the O_2 reduction flow through the external circuit from the anode, an equal magnitude oxidation reaction takes place ($2Pb + 2H_2O \rightarrow 2PbO + 4H^+ + 4e^-$). The resulting electric current yields an output signal that is linearly proportional to the O_2 concentration (0–100% vol.) surrounding the electrodes.

Table 1 – Biochemical reactions associated with aerobic microbial respiration in silage.		
Consummation	Respiration equations, chemical reaction and by-product	Microorganisms
Lactic acid	$CH_3CHOHCOOH + 3O_2 \rightarrow 3CO_2 + 3H_2O + 1368.2$ kJ mol^{-1}	Yeast, acetic acid bacteria
Acetic acid	$CH_3COOH + 2O_2 \rightarrow 2CO_2 + 2H_2O + 875.1$ kJ mol^{-1}	Acetic acid bacteria
Glucose	$C_6H_{12}O_6 + 6O_2 \rightarrow 6CO_2 + 6H_2O + 2870$ kJ mol^{-1}	Yeast, mould, lactic acid bacteria
Ethanol	$C_2H_5OH + O_2 \rightarrow CH_3COOH + H_2O + 492.6$ kJ mol^{-1}	Acetic acid bacteria
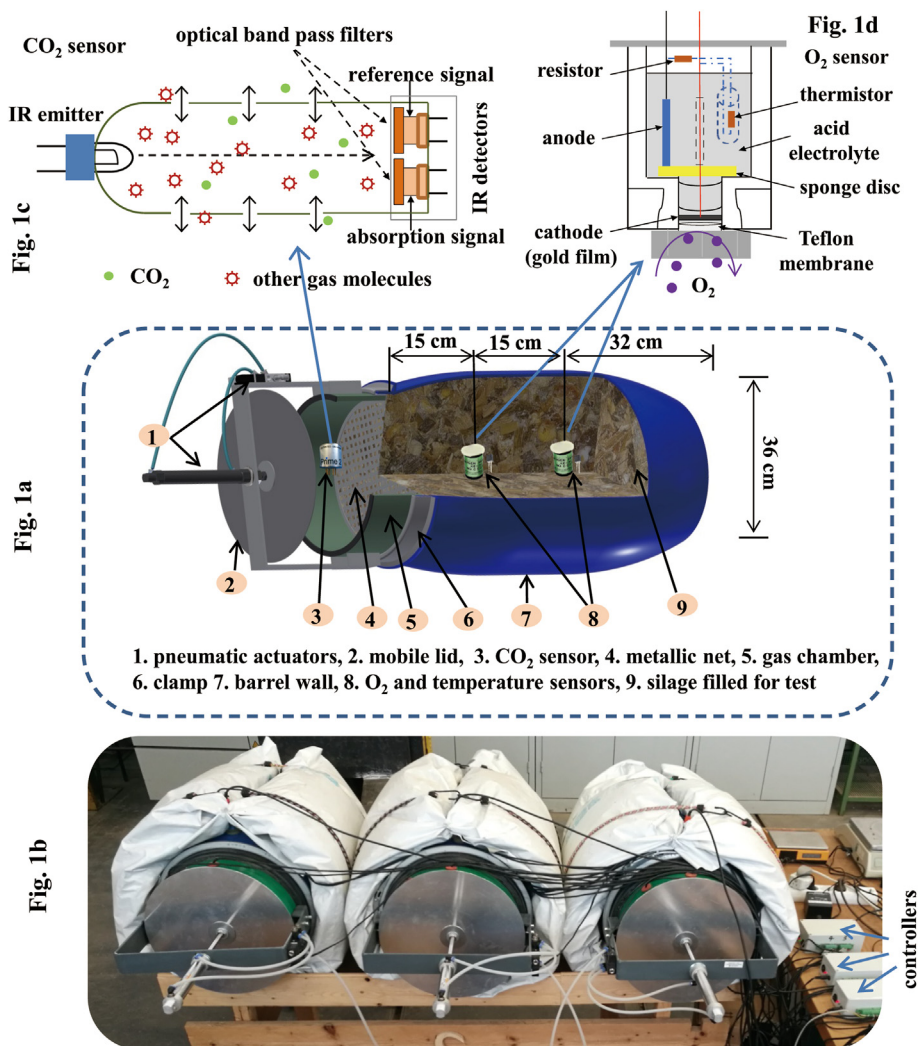
Fig. 1 — (a) The multi-sensor experimental cell with cut-away illustration shows two dual-sensors for measuring O_2 diffusion and aerobic reheating in silage, and a nondispersive infrared sensor for measuring CO_2 flux at the working face of the silage. (b) Three novel experimental cells combined with 3 mini-silos were tested *in situ* for evaluating antioxidant stability. (c) Schematic diagram of the nondispersive infrared CO_2 sensor integrated in the cell. (d) Schematic diagram of the electrochemical O_2 sensor integrated in the cell.

Table 2 — Technical information of the O_2, CO_2 and temperature sensors used.

Parameter	Sensor-type	Manufacturer	Range	Accuracy	Response(s)
Oxygen	KE-50	FIGARO Engineering Inc. Japan	0—100% (vol.)	±2 vol.% of full scale	60
Carbon dioxide	Prime 2	Clairair Ltd. UK	0—5% (vol.)	±3% of full scale	60
Temperature	DS18B20	Maxim Integrated. USA	−55 to 125 (°C)	±0.125 °C	<30

2.5. Silage crop and preparation

The crop material of the tested silage was triticale (var. Tender PZO) grown in the field (14.5 ha) in Rheinbach, Bonn, Germany (50°37′32″N, 6°56′57″W). The crop was seeded on October 5 2018 (165 kg ha^{-1}) and harvested on June 26 2019. Crop protection measures were applied as: herbicide, Herold (active ingredient (AI): Flufenacet and Diflufenican) 0.6 l ha^{-1} on 22 October, 2018, shortening of the stalk, Moddus (AI: Trinexapac-ethyl) 0.4 l ha^{-1} and fungicide, Diego (AI:

Thiophanate Methyl) 0.25 l ha^{-1} on February 27 2019, and fungicide, Capalo (AI: Metrafenone, Epoxiconazole and Fenpropimorph) 1.5 l ha^{-1} on May 6 2019. Fertilisation was applied as: biogas slurry, 15 m^3 ha^{-1} (120 kg N ha^{-1}) on February 12 2019, liquid nitrogen fertiliser, Nitroslow Fluid N 28, 30 l ha^{-1} (8.4 kg N ha^{-1}) on February 27 2019. The yield was 46 t fresh matter ha^{-1} and dry matter (DM) was 40% of fresh matter.

Immediately after harvest, the triticale crop was chopped (8-mm length) and packed as mini-silo form into six barrels at

190 kg m^{-3} DM (low density (LD) samples) and six barrels at 250 kg m^{-3} DM (high density (HD) samples), using a hydraulic press attached to a 34 cm diameter disk. Barrels were sealed to create anaerobic conditions for fermentation and storage. Aerobic stability of the silage samples was assessed following the experimental scheme of the German Agricultural Society (DLG, 2006; Pauly & Wyss, 2019). During the anaerobic storage phase, three barrels packed at LD and three at HD were opened for air exposure/stress for 24 h on July 24 and reopened on August 7 (i.e., 28- and 42-day after sealing). All measurements were conducted in both air-stressed and intact samples. The experiment started on day 50 after sealing (August 15, 2019), with 7 days of an experimental cycle. Prior to and after the experiment, 500 g samples were extracted from each barrel for determination of DM content (200 g), pH (50 g), organic acid (100 g), sugar (50 g) and microbial counts (100 g). The DM contents of the silage samples were 38%–41% (Table 3), determined by oven-drying at 70 °C for 48 h. pH was measured by extracting a 25 g subsample of the silage with 0.225 L deionised water for 30 min using a commercial pH sensor (BlueLine 21, pH, SI Analytic GmbH, Maize, Germany, measurement range 2–13 pH, allowable error ± 0.1 pH), according to the standard protocol for *ex situ* pH determination of silage (Junges, Schmidt, Novinski, & Pratti Danie, 2013; Woodard, Prine, & Bates, 1991).

2.6. Microbial and chemical analyses

Silage samples were divided into two aliquots, which were analysed in parallel. From each aliquot 30 g was suspended in 270 ml of ¼-strength ringer solution (2.25 g l^{-1} NaCl, 0.105 g l^{-1} KCl, 0.06 g l^{-1} CaCl$_2$, 0.05 g l^{-1} NaHCO$_3$; Merck, Darmstadt, Germany) and homogenised in a mixer for 1 min. From this suspension, total bacterial counts were analysed on plate-count agar (5.0 g l^{-1} enzymatic digest of casein, 2.5 g l^{-1} yeast extract, 1.0 g l^{-1} glucose, 15 g l^{-1} agar, pH = 7.0; Merck, Darmstadt, Germany) after aerobic incubation at 30 °C for two days. Lactic acid bacteria were quantified on MRS agar (Merck, Darmstadt, Germany) after anaerobic cultivation for 3 days at 30 °C. Yeasts and moulds were detected using yeast extract glucose chloramphenicol (YGC)-agar (5.0 g l^{-1} yeast extract, 20.0 g l^{-1} glucose, 0.1 g l^{-1} chloramphenicol, 14.9 g l^{-1} agar, pH = 6.6; Merck, Darmstadt, Germany) after incubation at 25 °C for three days.

Lactic and acetic acids were determined using high-performance liquid chromatography (HPLC; LC-2010AHT, Shimadzu Corp., Kyoto, Japan), coupled with an integrated UV-detector set at 210 nm. Calibration solutions for HPLC analysis were prepared by diluting L-lactic and acetic acid solutions with water to obtain working solutions of 2, 20, 40, 60, 80 and 100 mg L^{-1}. Glucose and fructose contents were determined with an enzymatic test at the onset and end of the experiment (both contents <3 g kg^{-1} DM). The microbial and chemical analyses were repeated and means are presented.

2.7. Statistical analysis

Experimental data were analysed using SPSS v25.0 (IBM Co., Armonk, NY, USA). Linear regression and curve fitting were evaluated using coefficient of determination (R^2) and significance (P) respectively. Two-way Analysis of Variance (ANOVA) was conducted for effects of experimental scheme (two treatment types, i.e. air-stress and intact), bulk density (two levels, i.e. 190 kg m^{-3} DM and 250 kg m^{-3} DM) and the interactions, on chemical and microbial compositions in the initial and final data and on the aerobic parameters, calculated from the measured results.

3. Results

3.1. Characteristics of triticale silage

The fermentation and aerobic deterioration characteristics, represented as the changes in chemical and microbial composition corresponding to the initial and final analysis, i.e. prior to and immediately after the experiment, are shown in Table 3. There was a significant effect of treatment on pH (P < 0.01), acetic acid (P < 0.05) and yeasts (P < 0.05) in the initial analysis. In the LD samples, the acetic acid content in air stressed samples was lower (P < 0.05) than in the intact samples. The air-stressed samples had higher (P < 0.05) yeast counts in the HD samples. The treatment of triticale silage (aerobic exposure) significantly influenced the levels of lactic acid (P < 0.01), acetic acid (P < 0.01) and ethanol (P < 0.05) in the final analysis. The bulk density of triticale silage also exerted a significant effect on the concentration of lactic acid (P < 0.01), ethanol (P < 0.01) and yeast (P < 0.01) after aerobic exposure. The interaction between treatment and bulk density was also significant for the amounts of both lactic acid (P < 0.01) and acetic acid (P < 0.01) in the final analysis. The air-stressed silage in LD had the lowest lactic acid concentration at the end of the experiment, demonstrating that lactic acid loss was greatest in this case. The air-stressed silage had lower acetic acid content than the intact silage. The intact silages with LD had the least ethanol, whereas that with HD had the lowest population of yeast.

3.2. Aerobic characteristics of O$_2$ and T$_{si}$

The time courses of O$_2$ and T$_{si}$ (Fig. 2) were recorded during aerobic exposure, at 15-cm and 30-cm behind the working face, in both LD and HD barrels/mini-silos. Each time-course represents an averaged data set of the three replicate samples. From these dynamic courses, four observations can be noted.

First, after the barrels/mini-silos were opened, initially O$_2$ could penetrate deeply into the silage because of the minimal activity of aerobic microorganisms (Pitt, 1986; Pitt & Muck, 1993; Sun et al., 2017). Oxygen diffusion dominated the O$_2$ concentration, which reached a peak (16–20% vol.) first at 15-cm and subsequently at 30-cm. In contrast to the variations of T$_{si}$, all peaks of O$_2$ concentration occurred when these samples remained aerobically stable (i.e. T$_{si}$ − T$_a$ < 2 °C) (Muck, 2004). The peak of O$_2$ revealed a dynamic balance between the O$_2$ mass introduced and microbial consumption at the measurement point.

Secondly, as the aerobic exposure progressed, the decline of the O$_2$ concentration indicated that the aerobic

Table 3 – Initial and final contents of organic acids, ethanol, yeasts and moulds in silage samples, determined from laboratory analyses.

Item	Bulk density	Treatment		SEM	Significance of effects		
		Air-stressed	Intact		Tr	B	Tr × B
Initial							
Dry matter (g kg^{-1} WW)	LD	397	385	11.392	NS	NS	NS
	HD	404	388				
pH	LD	4.0	3.9	0.029	**	NS	NS
	HD	4.0	3.9				
Lactic acid (g kg^{-1} DM)	LD	47.55	52.35	2.004	NS	NS	NS
	HD	48.96	52.32				
Acetic acid (g kg^{-1} DM)	LD	5.72^{B}	8.66^{A}	0.781	*	NS	NS
	HD	7.40	9.24				
Butyric acid (g kg^{-1} DM)	LD	<0.34	<0.34	–	–	–	–
	HD	<0.34	<0.34				
Ethanol (g kg^{-1} DM)	LD	8.7l5	8.89	0.201	NS	NS	NS
	HD	8.53	8.61				
Yeasts (log$_{10}$ cfu g^{-1} WW)	LD	6.58	6.02	0.286	*	NS	NS
	HD	6.70^{A}	5.33^{B}				
Moulds (log$_{10}$ cfu g^{-1} WW)	LD	<2	<2	–	–	–	–
	HD	<2	<2				
Final							
Dry matter (g kg^{-1} WW)	LD	409	410	3.041	NS	NS	NS
	HD	404	406				
pH	LD	4.2^{a}	4.1	0.041	NS	NS	NS
	HD	4.0^{b}	4.0				
Lactic acid (g kg^{-1} DM)	LD	25.86^{Bb}	34.93^{A}	1.025	**	**	**
	HD	36.25^{a}	34.77				
Acetic acid (g kg^{-1} DM)	LD	2.35^{Bb}	28.07^{Aa}	0.667	**	NS	**
	HD	7.31^{Ba}	22.97^{Ab}				
Butyric acid (g kg^{-1} DM)	LD	<0.33	<0.33	–	–	–	–
	HD	<0.33	<0.33				
Ethanol (g kg^{-1} DM)	LD	5.99^{A}	5.01^{Bb}	0.287	*	**	NS
	HD	6.98	6.41^{a}				
Yeasts (log$_{10}$ cfu g^{-1} WW)	LD	8.11	7.99^{a}	0.103	NS	**	NS
	HD	7.74^{A}	7.45^{Bb}				
Moulds (log$_{10}$ cfu g^{-1} WW)	LD	<2	<2	–	–	–	–
	HD	<2	<2				

$^{A, B}$ values with different superscripts within treatment differ (P < 0.05).
$^{a, b}$ values with different superscripts within bulk density differ (P < 0.05).
WW, wet mass; DM, dry matter; cfu, colony-forming units; SEM, standard error of the mean; Tr, treatment (air-stress or intact); B, bulk density (LD or HD); *P < 0.05; **P < 0.01; NS, not significant.

microorganisms of the silage multiplied sufficiently that the microbial consumption exceeded the O$_2$ mass introduced (Muck & Pitt, 1994; Sun et al., 2015, 2017). A lag of the O$_2$ decrease between 15- and 30-cm depths in each subfigure demonstrated that variation in microbial activity was both temporal and spatial, reflecting the length of the diffusion path/time for O$_2$.

Thirdly, unlike the dramatic rise of O$_2$, T$_{si}$ initially remained insensitive to opening of the barrels (i.e. aerobically stable), and then increased rapidly after the O$_2$ peaks were reached. The arrows and labels in Fig. 2 denote the aerobic stability of the silage samples that was defined as the time (h) required for T$_{si}$ (at 15-cm or 30-cm) to reach 2 °C above ambient (Muck, 2004).

Lastly, the air-stress treatment and the low density packing significantly advanced the starting times of the T$_{si}$-rise and O$_2$-decline at each point monitored, i.e. both reduced the aerobic stability of these samples.

3.3. Aerobic characteristics of CO$_2$ flux

The time courses of CO$_2$ flux are presented with respect to LD (Fig. 3a) and HD samples (Fig. 3b). To facilitate the direct comparison of the CO$_2$ flux with the T$_{si}$-defined aerobic stability (Fig. 2), the timing (arrow) and the time (h) at which T$_{si}$ reached 2 °C above ambient are also shown in Fig. 3. All time courses of CO$_2$ flux exhibit similar dynamics, a drop-and-rise in the initial 3- or 4-days and then stabilisation. According to Fick's second law, the rise revealed an increasing concentration of CO$_2$ in the silage. The stable CO$_2$ flux in the final 3- or 4-days indicated a balance between production of CO$_2$ and its diffusion under a stable concentration gradient (Fick's first law). The large initial fluxes with the subsequent declines at the onset of the experiment (0 < t < 24 h) were caused by discharge of the CO$_2$ by-products of anaerobic fermentation accumulated in the sealed barrels. Of this, an observable line of evidence is that the initial T$_{si}$ for all samples remained
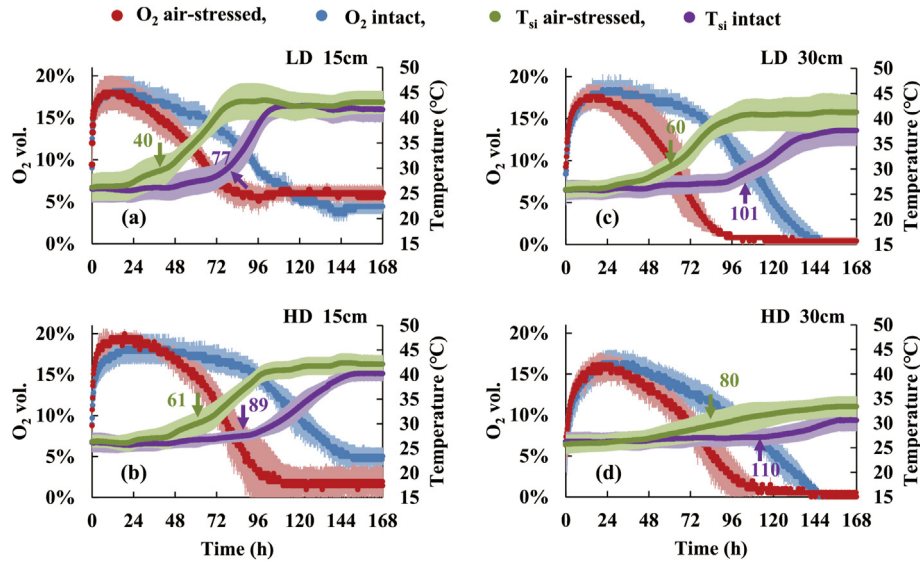
Fig. 2 − Dual-factor data stream showing simultaneous time courses of T_{si} and O_2 in response to aerobic exposure, measured at 15 cm behind the working face, a) packed at low density (LD, 190 kg m^{-3} DM) or b) at high density (HD, 250 kg m^{-3} DM); and at 30-cm behind the working face, c) at LD or d) HD. The arrows and labels denote the aerobic stability of the silage samples that was defined as the time (h) required for T_{si} (15-cm or 30-cm) to reach 2 °C above ambient.
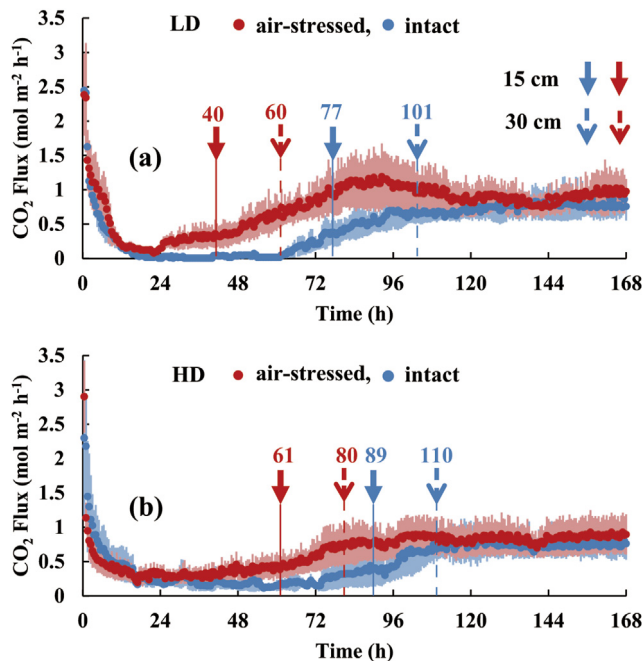
Fig. 3 − Time courses of CO_2 flux measured at the working faces of the air-exposed and intact mini-silos packed a) at LD and b) HD. The arrows and labels denote the aerobic stability of the silage samples that was defined as the time (h) required for T_{si} (15-cm or 30-cm) to reach 2 °C above ambient.

aerobically stable ($\Delta T_{si} \leq 0.7$ °C, $0 < t < 24$ h, Fig. 2) during the discharging period. The CO_2 discharging from 2.5−3 mol m^{-2} h^{-1} to 0.1 mol m^{-2} h^{-1} for all samples lasted less than 24 h, while the aerobic stabilities of all samples persisted from 40−110 h. The rise of CO_2 flux from the air-stressed

samples occurred earlier than in the intact samples, in both LD and HD barrels (Fig. 3).

Figure 4 shows the daily emissions of CO_2 per kg DM from the LD (Fig. 4a) and HD (Fig. 4b) barrels, calculated from the time courses of CO_2 flux (Fig. 3) using Eq. (2). The data of day-1 were excluded since they were independent of aerobic deterioration. The daily fluxes of CO_2 from the HD mini-silos of day-2 for both the air-stressed and intact samples were slightly greater than those released from the LD mini-silos. This is likely to be because silage with higher density had more dry matter under the same levels of water content so that on opening more solid components were exposed directly to air, resulting in greater production of CO_2. However, as oxygen diffused gradually into the silage through the working face, the daily fluxes of CO_2 from LD barrels exceeded those from the HD barrels, indicating that the LD samples had higher porosity and higher diffusion coefficient. For the air-stressed samples, the peaks of CO_2 flux from the LD barrels appeared on day-4 and from the HD barrels on day-5. Table 4 demonstrates that the total aerobic production of CO_2 over the entire experiment was greater from the air-stressed samples than from the intact samples in LD, with less effect in HD.

3.4.   Interrelation of the aerobic parameters

These results suggest that the three parameters all reflect the progress of aerobic degradation. The regression analysis (Fig. 5) provides insight into the interrelation of T_{si}, O_2 concentration (both at 15 cm) and CO_2 flux. The relationship between T_{si} (27−44 °C) and O_2 (2−18% vol.) was highly linear ($0.982 \leq R^2 \leq 0.994$) with negative slope (Table 5), whereas that between T_{si} (27−44 °C) and CO_2 (0.01−1.2 mol m^{-2} h^{-1}) was also linear ($0.711 \leq R^2 \leq 0.981$) but with positive slope (Table 5). Similarly, at 30 cm, the regression of O_2 on T_{si} (Fig. 6) increased linearly with the consumption of O_2 in LD ($0.948 \leq R^2 \leq 0.967$,
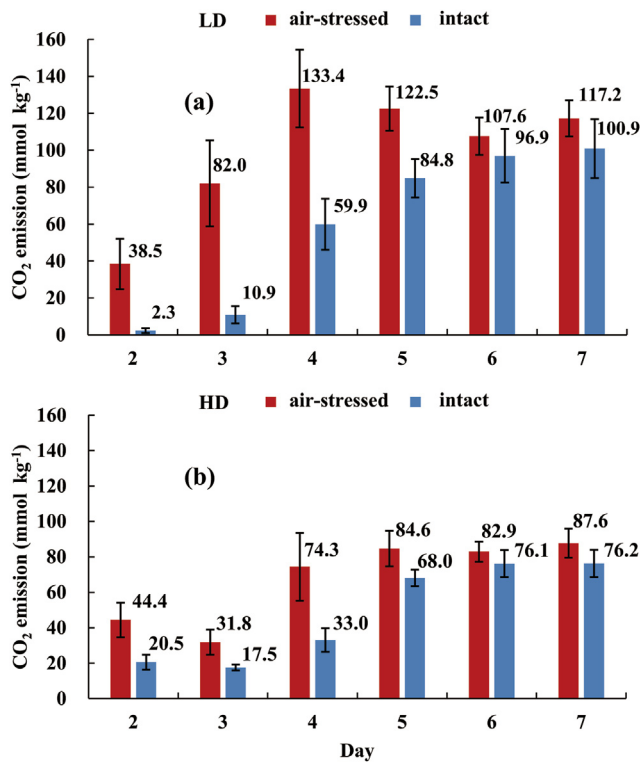
Fig. 4 − Daily aerobic production of CO_2 from the air-stressed and intact mini-silos packed at a) LD and b) HD.

Table 5). The T_{si} at 30 cm in the HD barrels only rose from 27 °C to 33 °C (air-stressed silage, Fig. 6c) or 30 °C (intact sample, Fig. 6d), and in both cases T_{si} was still highly linear with the consumption of O_2 ($0.815 \leq R^2 \leq 0.932$, Table 5). For all samples at 30 cm, the relationship between T_{si} (27−41 °C) and CO_2 (0.01−1.2 mol m^{-2} h^{-1}) remained linear with R^2 from 0.464 to 0.901 (Table 5).

In contrast to the observations at 15 cm (Fig. 5), effects of silage density and the distance from the working face to the measurement points can be seen more clearly at 30 cm (Fig. 6). The higher R^2 of T_{si} vs. O_2 is likely to be because both parameters were measured at the same points in the silage. The excellent linear relationship demonstrated that T_{si} and O_2 consumption varied at the same rate following AMR. The

relatively lower R^2 between T_{si} and CO_2 may have two causes. First, the CO_2 flux was measured from the complete working face of each barrel, but T_{si} was from a point measurement at 15 or 30 cm behind the working face. Second, there was a time lag as CO_2 diffused out of the working face, depending on path length, the concentration gradient of the CO_2 and the specific diffusion coefficient of the silage, according to Fick's laws.

4. Discussion

Our experiment demonstrated that all parameters suggested as aerobic indicators of AMR of silage were trackable, using available temperature, oxygen and carbon-dioxide sensors. Although the T_{si}-related definition of aerobic stability has been widely applied (Borreani et al., 2018; Pahlow et al., 2003; Wilkinson & Davies, 2013), a similar definition using O_2 or CO_2 is still to be developed.

On the technical side, continuous measurement of T_{si} has become simple and inexpensive. However, these T_{si}-data measured at the two depths (Fig. 2) reflected deterioration information in limited volumes of the silage. Due to the uneven distribution pattern of T_{si} in large on-farm silos, Borreani and Tabacco (2010) suggested the temperature of the central zone of the silo to be the reference temperature. The temperature difference related to the reference was then used as a heating index associated with aerobic deterioration. In addition to the spatial variability of T_{si} in silage, the ambient temperature fluctuates diurnally (Borreani & Tabacco, 2010; Okatsu, Swanepoel, Maga, & Robinson, 2019; Robinson & Swanepoel, 2016). This may interfere with determining the threshold of aerobic stability that is defined as the temperature difference between the silage and ambient. Thus, to precisely determine the aerobic stability for farm silos further extended studies are required.

The O_2 pattern was also obtained from point-measurements, reflecting the site-specific and temporal activities of the aerobic microorganisms in silage (Green et al., 2012; Pitt, 1986; Pitt & Muck, 1993; Sun et al., 2015, 2017). Our study, relying on the simultaneous and continuous measurements of O_2 and T_{si} over time using the dual-sensor technique, first reported the excellent linear relationship of these parameters (Figs. 5, 6) as the dual responses to aerobic

---

Table 4 − Aerobic indicators calculated from the measured parameters: the decline of O_2 concentration (% vol.) from the initial maximum (T_{si}-stable) to the value measured when T_{si} reached 2 °C above ambient temperature, and the total aerobic production of CO_2.

Item	Bulk density	Treatment		SEM	Significance of effects		
		air-stress	Intact		T	B	T × B
Decline of O_2 at 15 cm (% vol.)	LD	3.8	5.3[a]	1.4	NS	NS	NS
	HD	6.1	2.9[b]				
Decline of O_2 at 30 cm (% vol.)	LD	7.8	7.1	1.3	NS	NS	NS
	HD	10.7	7.7				
CO_2 production (mmol kg^{-1} DM)	LD	601[A]	356[B]	50.5	**	*	NS
	HD	406	291				

[A, B] values with different superscripts within treatment differ (P < 0.05).
[a, b] values with different superscripts within bulk density differ (P < 0.05).
SEM, standard error of the mean; Tr, treatment (air-stress or intact); B, bulk density (LD or HD); *P < 0.05; **P < 0.01; NS, not significant.
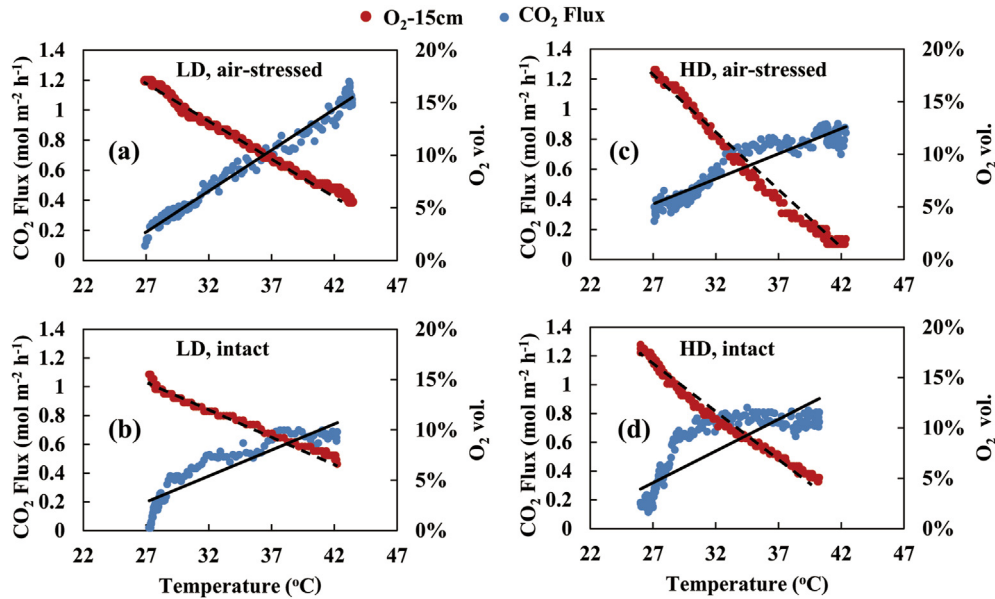
Fig. 5 – Relationships between T_{si} and both volumetric concentration of O_2 (red symbols) and CO_2 flux (blue symbols), where both T_{si} and O_2 were measured at 15 cm behind the working face. a) air-stressed mini-silos and b) intact mini-silos packed at LD; and c) air-stressed mini-silos and d) intact mini-silos packed at HD. The dotted line refers to the linear regression of T_{si} and O_2, and the solid line to that of T_{si} and CO_2. All resulting regression equations are listed in Table 5. (For interpretation of the references to colour in this figure legend, the reader is referred to the Web version of this article.)

Table 5 – The slope (k_0), intercept (k_1), coefficient of determination (R^2) and significance (P) of those regressions showed in Figs. 5 and 6

$y = k_0 x + k_1$	k_0	k_1	R^2	P	$y = k_0 x + k_1$	k_0	k_1	R^2	P
Figure 5									
(a) $T_{si}\{^{O_2}_{CO_2}$	−0.007	0.351	0.994	<0.01	(c) $T_{si}\{^{O_2}_{CO_2}$	−0.011	0.479	0.990	<0.01
	0.055	−1.285	0.981	<0.01		0.034	−0.536	0.886	<0.01
(b) $T_{si}\{^{O_2}_{CO_2}$	−0.005	0.284	0.984	<0.01	(d) $T_{si}\{^{O_2}_{CO_2}$	−0.009	0.415	0.982	<0.01
	0.036	−0.779	0.825	<0.01		0.044	−0.873	0.711	<0.01
Figure 6									
(a) $T_{si}\{^{O_2}_{CO_2}$	−0.012	0.460	0.967	<0.01	(c) $T_{si}\{^{O_2}_{CO_2}$	−0.022	0.706	0.932	<0.01
	0.059	−1.235	0.901	<0.01		0.079	−1.712	0.833	<0.01
(b) $T_{si}\{^{O_2}_{CO_2}$	−0.015	0.544	0.948	<0.01	(d) $T_{si}\{^{O_2}_{CO_2}$	−0.038	1.137	0.815	<0.01
	0.047	−0.858	0.569	<0.01		0.132	−3.154	0.464	<0.01

exposure. This finding suggests that a promising O_2-index may be developed to characterise the aerobic stability of silage, similar to that of T_{si}. Based on the paired measurements of T_{si} and O_2 concentration in Fig. 2 we present Table 4 to show the drops of O_2 concentration ($\Delta O_2 = 2.9-10.7\%$ vol., n = 24) between the initial maximum values during the T_{si}-stable period and the values measured when T_{si} reached 2 °C above ambient (T_a). These new data with considerable discrepancy of ΔO_2 also suggests exploring different indices to assess the antioxidation ability of silage.

Silage is a CO_2-rich porous medium before feed-out (Ashbell et al., 1991; Ashbell et al., 2002; Filya, 2003; Honig, 1990; Weinberg & Ashbell, 1994; Weinberg et al., 2009). On the other hand, few studies have noted that the CO_2 previously accumulated from anaerobic fermentation in silage is a type of noise that may confound the interpretation of CO_2 flux after opening the silage. Our study not only found this

(Fig. 3) with the direct evidence of the initial $\Delta T_{si} \leq 0.7$ °C within 0–24 h (Fig. 2), but also showed that the CO_2 flux is a simple indicator of aerobic deterioration after the initial CO_2 discharge is complete, and remained minimal during the initial aerobically stable phase (i.e. the period of $\Delta T_{si} \leq 2$ °C). In the case of the relatively poor aerobic stability that is shorter than the discharge time of carbon dioxide, the CO_2 flux has to be partitioned with a two-pool model, i.e. anaerobic and aerobic pools (Shan et al., 2019). In addition, our previous study (Li et al., 2017) found that CO_2 produced in the silage was partially dissolved by the silage water. Here the significant discharge of CO_2 at the onset of the experiment demonstrated that the water in the silage was fully saturated with dissolved CO_2 before these mini-silos opened. Therefore, the measured CO_2 flux directly reflected the aerobic production during feed-out when the day-1 data of CO_2 flux were excluded.
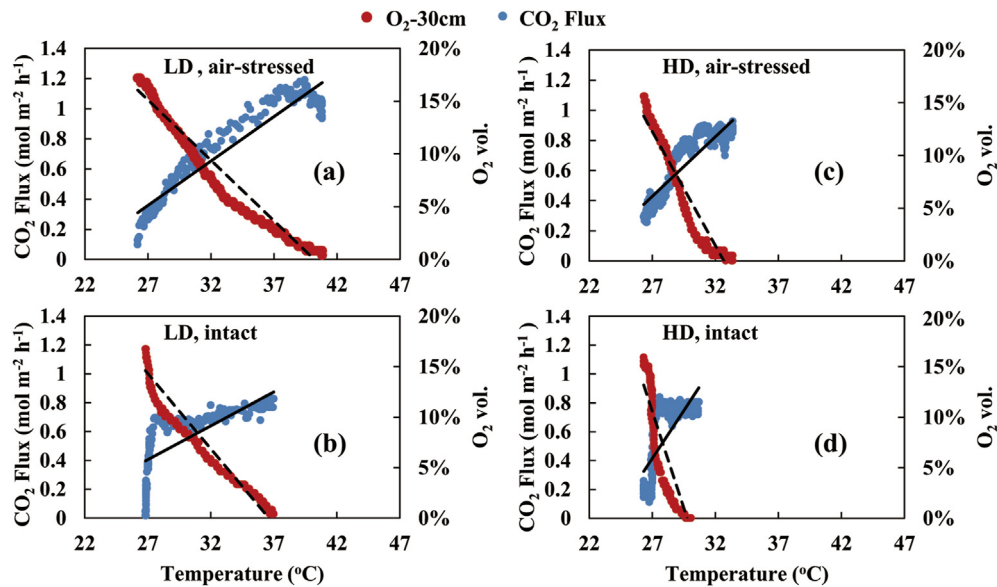
Fig. 6 — Relationships between T_{si} and both volumetric concentration of O_2 (red symbols) and CO_2 flux (blue symbols), where both T_{si} and O_2 measured at 30 cm behind the working face. a) air-stressed mini-silos and b) intact mini-silos packed at the LD; and c) air-stressed mini-silos and d) intact mini-silos packed at the HD. The dotted line refers to the linear regression of T_{si} and O_2, and the solid line to that of T_{si} and CO_2. All resulting regression equations are listed in Table 5. (For interpretation of the references to colour in this figure legend, the reader is referred to the Web version of this article.)

5. Conclusions

Using our advanced multi-sensor technique, we successfully characterised the aerobic time courses of O_2 influx, CO_2 outflow and T_{si} during feed-out of triticale silage, and provide the first reports of the interrelations among these parameters. These findings are explicitly related to the degradation process by AMR. The strong linear relationship between T_{si} and O_2 demonstrated that the consumption of oxygen, aerobic reheating and microbial activity in these silage samples had similar temporal rates and occurred simultaneously. Moreover, by comparison with the measurements of aerobic stability, we showed that CO_2 flux was dominated by anaerobic discharge in the stable phase and aerobic real-time production in the unstable phase. Therefore, the CO_2 flux measured, after the initial out-gassing, can be used as an indicator of aerobic deterioration. For the O_2- and CO_2-related definitions of aerobic stability of silage, future studies with different silage materials and robust metrics are expected.

Declaration of competing interest

The authors declare that they have no known competing financial interests or personal relationships that could have appeared to influence the work reported in this paper.

Acknowledgement

REFERENCES

Ashbell, G., Weinberg, Z. G., Azrieli, A., Hen, Y., & Horev, B. (1991). A simple system to study the aerobic determination of silages. *Canadian Agricultural Engineering, 34*, 171—175.

Ashbell, G., Weinberg, Z. G., Hen, Y., & Filya, I. (2002). The effects of temperature on the aerobic stability of wheat and corn silages. *Journal of Industrial Microbiology and Biotechnology, 28*(5), 261—263.

Bernardes, T. F., Daniel, J. L. P., Adesogan, A. T., McAllister, T. A., Drouin, P., Nussio, L. G., et al. (2018). Silage review: Unique challenges of silages made in hot and cold regions. *Journal of Dairy Science, 101*(5), 4001—4019.

Borreani, G., & Tabacco, E. (2010). The relationship of silage temperature with the microbiological status of the face of corn silage bunkers. *Journal of Dairy Science, 93*(6), 2620—2629.

Borreani, G., Tabacco, E., Schmidt, R. J., Holmes, B. J., & Muck, R. E. (2018). Silage review: Factors affecting dry matter and quality losses in silages. *Journal of Dairy Science, 101*(5), 3952—3979.

Courtin, M. G., & Spoelstra, S. F. (1990). A simulation model of the microbiological and chemical changes accompanying the initial stage of aerobic deterioration of silage. *Grass and Forage Science, 45*(2), 153—165.

DLG. (2006). *Grobfutterbewertung-Teil B.-DLG-Schlüssel zur Beurteilungder Gärqualität von Grünfuttersilagen auf Basis der chemischen Untersuchung. DLG-Information 2/2006*. Germany: DLG, Frankfurt a.M.

Filya, I. (2003). The effect of lactobacillus buchneri and lactobacillus plantarum on the fermentation, aerobic stability, and ruminal degradability of low dry matter corn and sorghum silages. *Journal of Dairy Science, 86*(11), 3575–3581.

Green, O., Bartzanas, T., Løkke, M. M., Bochtis, D. D., Sørensen, C. G., Jørgensen, O. J., et al. (2012). Spatial and temporal variation of temperature and oxygen concentration inside silage stacks. *Biosystem Engineering, 111*(2), 155–165.

Herrmann, C., Idler, C., & Heiermann, M. (2015). Improving aerobic stability and biogas production of maize silage using silage additives. *Bioresource Technology, 197*, 393–403.

Herrmann, C., Prochnow, A., & Heiermann, M. (2011). Influence of chopping length on capacities, labour time requirement and costs in the harvest and ensiling chain of maize. *Biosystems Engineering, 110*(3), 310–320.

Honig, H. (1990). Evaluation of aerobic stability. In *Grass and forage reports. Proceedings of the Eurobac conference, Uppsala, Sweden* (pp. 76–82).

Jatkauskas, J., Vrotniakiene, V., Ohlsson, C., & Lund, B. (2013). The effects of three silage inoculants on aerobic stability in grass, clover-grass, lucerne and maize silages. *Agricultural and Food Science, 22*(1), 137–144.

Johnson, L. M., Harrison, J. H., Davidson, D., Mahanna, W. C., Shinners, K., & Linder, D. (2002). Corn silage management: Effects of maturity, inoculation, and mechanical processing on pack density and aerobic stability. *Journal of Dairy Science, 85*(2), 434–444.

Junges, D., Schmidt, P., Novinski, C. O., & Pratti Danie, J. L. (2013). Additive containing homo and heterolactic bacteria on the fermentation quality of maize silage. *Acta Scientiarum. Animal Sciences, 35*(4), 371–377.

Kristensen, N. B., Sloth, K. H., HøJberg, O., Spliid, N. H., Jensen, C., & ThøGersen, R. (2010). Effects of microbial inoculants on corn silage fermentation, microbial contents, aerobic stability, and milk production under field conditions. *Journal of Dairy Science, 93*(8), 3764–3774.

Kung, L., Shaver, R. D., Grant, R. J., & Schmidt, R. J. (2018). Silage review: Interpretation of chemical, microbial, and organoleptic components of silages. *Journal of Dairy Science, 101*(5), 4020–4033.

Lee, S. J., Hanna, M. A., & Bullerman, L. B. (1986). Carbon dioxide and aflatoxin production in high-moisture corn treated with potassium sorbate. *Cereal Chemistry, 63*(2), 82–84.

Li, M., Shan, G., Zhou, H., Buescher, W., Maack, C., Jungbluth, K. H., et al. (2017). CO_2 production, dissolution and pressure dynamics during silage production: Multi-sensor-based insight into parameter interactions. *Scientific Reports, 7*(14721), 1–9.

McEniry, J., Forristal, P. D., & O'Kiely, P. (2011). Gas composition of baled grass silage as influenced by the amount, stretch, colour and type of plastic stretch-film used to wrap the bales, and by the frequency of bale handling. *Grass and Forage Science, 66*(2), 277–289.

Muck, R. E. (2004). Effects of corn silage inoculants on aerobic stability. *Transactions of the ASAE, 47*(4), 1011–1016.

Muck, R. E., & Pitt, R. E. (1994). Aerobic deterioration in corn silage relative to the silo face. *Transactions of the ASAE, 37*(3), 735–743.

Okatsu, Y., Swanepoel, N., Maga, E. A., & Robinson, P. H. (2019). Impacts of some factors that effect spoilage of silage at the periphery of the exposed face of corn silage piles. *Animal Feed Science and Technology, 247*, 234–247.

Pahlow, G., Muck, R. E., Driehuis, F., Elferink, S. J. O., & Spoelstra, S. F. (2003). Microbiology of ensiling. *Silage science and technology, 42*, 31–93.

Pauly, T., & Wyss, U. (2019). Efficacy testing of silage additives—methodology and existing schemes. *Grass and Forage Science, 74*(2), 201–210.

Pitt, R. E. (1986). Dry matter losses due to oxygen infiltration in silos. *Journal of Agricultural Engineering Research, 35*(3), 193–205.

Pitt, R. E., & Muck, R. E. (1993). A diffusion model of aerobic deterioration at the exposed face of bunker silos. *Journal of Agricultural Engineering Research, 55*(1), 11–26.

Ranjit, N. K., & Kung, L. (2000). The effect of lactobacillus buchneri, lactobacillus plantarum, or a chemical preservative on the fermentation and aerobic stability of corn silage. *Journal of Dairy Science, 83*(3), 526–535.

Robinson, P. H., & Swanepoel, N. (2016). Impacts of a polyethylene silage pile underlay plastic with or without enhanced oxygen barrier (EOB) characteristics on preservation of whole crop maize silage, as well as a short investigation of peripheral deterioration on exposed silage faces. *Animal Feed Science and Technology, 215*, 13–24.

Schwendenmann, L., & Macinnis-Ng, C. (2016). Soil CO_2 efflux in an old-growth southern conifer forest (agathis australis) – magnitude, components and controls. *Soil, 2*(3), 403–419.

Shan, G., Buescher, W., Maack, C., Zhou, H., & Sun, Y. (2019). An automatic smart measurement system with signal decomposition to partition dual-source CO_2 flux from maize silage. *Sensors and Actuators B: Chemical, 300*, 127053.

Shan, G., Sun, Y., Li, M., Jungbluth, K. H., Maack, C., Buescher, et al. (2016). An assessment of three different in situ oxygen sensors for monitoring silage production and storage. *Sensors, 16*(1), 91.

Sun, Y., Li, M., Cheng, Q., Jungbluth, K. H., Maack, C., Buescher, W., et al. (2015). Tracking oxygen and temperature dynamics in maize silage-novel application of a Clark oxygen electrode. *Biosystems Engineering, 139*, 60–65.

Sun, Y., Li, M., Zhou, H., Shan, G., Cheng, Q., Jungbluth, K. H., et al. (2017). In situ measurements and simulation of oxygen diffusion and heat transfer in maize silage relative to the silo surface. *Computers and Electronics in Agriculture, 137*, 1–8.

Weinberg, Z. G., & Ashbell, G. (1994). Changes in gas composition in corn silages in bunker silos during storage and feedout. *Canadian Agricultural Engineering, 36*(3), 155–158.

Weinberg, Z. G., Chen, Y., & Solomon, R. (2009). The quality of commercial wheat silages in Israel. *Journal of Dairy Science, 92*(2), 638–644.

Weiss, K., Kroschewski, B., & Auerbach, H. (2016). Effects of air exposure, temperature and additives on fermentation characteristics, yeast count, aerobic stability and volatile organic compounds in corn silage. *Journal of Dairy Science, 99*(10), 8053–8069.

Wilkinson, J. M., & Davies, D. R. (2013). The aerobic stability of silage: Key findings and recent developments. *Grass and Forage Science, 68*(1), 1–19.

Wilkinson, J. M., & Muck, R. E. (2019). Ensiling in 2050: Some challenges and opportunities. *Grass and Forage Science, 74*(2), 178–187.

Williams, A. G., Hoxey, R. P., & Lowe, J. F. (1997). Changes in temperature and silo gas composition during ensiling, storage and feeding-out grass silage. *Grass and Forage Science, 52*(2), 176–189.

Woodard, K. R., Prine, G. M., & Bates, D. B. (1991). Silage characteristics of elephantgrass as affected by harvest frequency and genotype. *Agronomy Journal, 83*(3), 245–247.